THE JOURNAL OF PHYSICAL CHEMISTRY Letters

Perspective

Cite This: J. Phys. Chem. Lett. 2019, 10, 2629−2640

pubs.acs.org/JPCL

Reducing Defects in Halide Perovskite Nanocrystals for Light-Emitting Applications

Xiaopeng Zheng,[†,∥] Yi Hou,[‡,∥] Hong-Tao Sun,[§] Omar F. Mohammed,[†] Edward H. Sargent,*[,‡] and Osman M. Bakr*[,†]

[†]Division of Physical Sciences and Engineering, King Abdullah University of Science and Technology (KAUST), Thuwal 23955-6900, Kingdom of Saudi Arabia

[‡]Department of Electrical and Computer Engineering, University of Toronto, 10 King's College Road, Toronto, Ontario M5S 3G4, Canada

[§]College of Chemistry, Chemical Engineering and Materials Science, Soochow University, Suzhou 215123, China

ABSTRACT: The large specific surface area of perovskite nanocrystals (NCs) increases the likelihood of surface defects compared to that of bulk single crystals and polycrystalline thin films. It is thus crucial to comprehend and control their defect population in order to exploit the potential of perovskite NCs. This Perspective describes and classifies recent advances in understanding defect chemistry and avenues toward defect density reduction in perovskite NCs, and it does so in the context of the promise perceived in light-emitting devices. Several pathways for decreasing the defect density are explored, including advanced NC syntheses, new surface-capping strategies, doping with metal ions and rare earths, engineering elemental compensation, and the translation of core−shell heterostructures into the perovskite materials family. We close with challenges that remain in perovskite NC defect research.

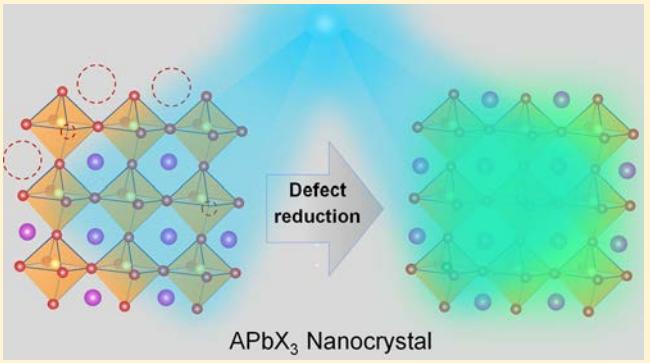

Colloidal perovskite nanocrystals (NCs) with tunable bandgaps, high photoluminescence quantum yields (PLQYs), facile synthesis, and narrow emission line widths are emerging as a new light-emitting technology for displays, light-emitting diodes (LEDs), and scintillators.[1−9] External quantum efficiencies (EQEs) of both red and green LEDs reached 20%, while scintillators based on perovskite NCs are also highly sensitive, with a detection limit ∼400 fold less than the standard dosage in medical imaging.[3,10−13] Perovskite NCs benefit from an ionic structure and low crystallization temperature, and thus are readily synthesized via low-cost solution processes. Their PL is also tunable from the ultraviolet (UV) to near-infrared, which bodes well for achieving Rec. 2020 standard by changing halide composition or NC size.[14−16] The resulting perovskite NC inks allow for multiple thin-film processing methods such as spin-coating and large-area roll-to-roll printing, which are potentially compatible with the procedures developed by display manufacturers (e.g., Sony, Samsung, and LG) for CdSe- or InP-based NCs to achieve fast, scalable and cost-effective panel production.[17−19]

Exciton binding energies (E_B) with relatively small values varying from 2 to 80 meV at room temperature were observed in 3D perovskites ($MAPbI_3$ and $MAPbBr_3$). The small E_B values of 3D perovskites render them essentially nonexcitonic materials, which is beneficial for solar cells but detrimental to light-emitting applications.[20−22] By utilizing NCs, one may achieve spatial confinement of electrons and holes within a limited volume of the NCs and, thereby, increase the E_B and promote radiative recombination rates, which is a crucial advantage of NCs over large-grain-sized polycrystalline films for light-emitting applications.[23−25] Perovskite NCs are a very mature system, offering tunable NC sizes reaching down to the exciton bohr radius and abundant ligand-exchanging prototypes.[1,12,26] However, the trap state density is higher in NCs than in polycrystalline films/single-crystals because of the dramatically increased surface area and number of dangling bonds, which trap a fraction of carriers without emitting light, and thus imposes severe limitations on device performance.[27,28] To enhance radiative recombination rates and reduce nonradiative ones induced by defect states, many efforts have been made to defect engineering by removing or filling trap states in perovskite NCs. Despite significant research efforts, many of the finer details of defect passivation mechanisms for perovskite NCs remain obscure. It is therefore necessary to summarize the existing strategies for passivating defects in perovskite NCs to further improve perovskite NCs-based light-emitting applications. Here, we review the advances concerning defect passivation rules, summarize the passivation strategies for perovskite NCs

Received: March 11, 2019
Accepted: April 30, 2019
Published: April 30, 2019

DOI: 10.1021/acs.jpclett.9b00689
J. Phys. Chem. Lett. 2019, 10, 2629−2640

Despite significant research efforts, many of the finer details of defect passivation mechanisms for perovskite NCs remain obscure. It is therefore necessary to summarize the existing strategies for passivating defects in perovskite NCs to further improve perovskite NCs-based light-emitting applications.

and provide a perspective on avenues for making further progress.

In 2015, Protesescu et al. synthesized nearly monodisperse $CsPbX_3$ nanocubes with high photoluminescence quantum yield.[29] The hot-injection method with reaction temperature of 140−200 °C yields monodisperse NCs; the size of NCs can be adjusted by varying both reaction temperature and thermodynamic equilibrium. Dong et al. demonstrated an effective way to synthesize uniform sized NCs by operating under thermodynamic equilibrium (Figure 1a).[30]

The effect of reaction temperatures between 180 and 250 °C on $CsPbCl_3$ and $CsPbBr_3$ NCs was investigated by Dutta et al. At higher temperature (250 °C), they observed a phase change quickly occurring, and cubes of $CsPbCl_3$ were exclusively formed and the PLQY was dramatically enhanced. At low temperatures (<160 °C), it was noted that the competition for the A sites of the perovskite crystals, between the ammonium and Cs ions, preferentially led to 2D layered perovskites as well as 3D perovskites.[31] It is believed that an alkylammonium ion resides on the surface Cs atoms in the NCs. Moreover, the use of excess halides during the reaction prevented the leach of halides from the NCs during annealing at high temperatures. The X-ray diffraction (XRD) data showed that without the addition of ammonium chloride salts the phase of $CsPbBr_3$ NCs transitioned to tetragonal, whereas with oleylammonium salt the phase remained orthorhombic. The wide-band gap $CsPbCl_3$ NCs, which were reported to be poorly emissive compared with $CsPbBr_3$, could achieve an absolute quantum yield of ∼51%.[32] $CuCl_2$ has been applied as an additive for high-temperature synthetic protocols to yield high-quality $CsPbCl_3$ NCs. While no further enhancement in PL intensity was observed following the addition of metal chloride postsynthesis, the PL intensity of pristine $CsPbCl_3$ was significantly enhanced after the postsynthesis treatment. That finding indicates that adding $CuCl_2$ minimized the chloride deficiency (i.e., reduced Cl vacancies) in the NCs.[33]

NCs containing bare Br or I exhibited PLQYs over 90%. However, the mixed halide compositions ($CsPbBr_xCl_{3-x}$) have shown much lower PLQY's (only 10−25%) (Figure 1b).[34] In such perovskites, Cl vacancies (V_{Cl}) lead to the formation of deep trap energy levels, which in turn cause severe nonradiative recombination.[35] Moreover, the defect formation energies are highly sensitive to composition. The defect deformation energy in $FAPbI_3$, for example, varies appreciably when partially substituting Cs/MA and Br for FA and I. The formation energy of PbI_2 vacancy increases by over a factor of 3 from the original value of ∼0.25 eV for a vacancy density of $\sim 3 \times 10^{17}$ cm^{-3}. That translates to a reduction in the vacancy concentration by a factor of approximately 10^9.[36]

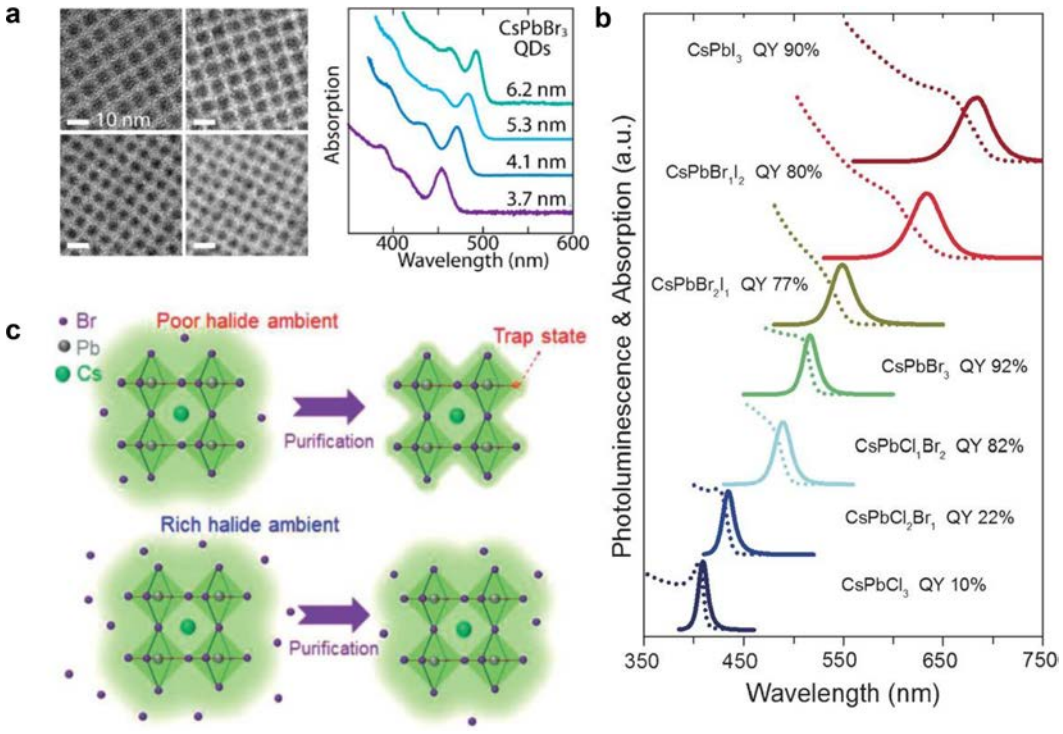

Figure 1. (a) Size control of $CsPbX_3$ NCs leading to highly uniform ensembles by thermodynamic equilibrium. Reprinted with permission from ref 30. Copyright 2018 American Chemical Society. (b) UV−vis and PL spectrum and PLQYs of $CsPbX_3$ NCs. Dashed and solid lines represent for PL and UV−vis spectrum, respectively. Adapted from ref 34. Copyright 2016 Wiley-VCH. (c) Schematics of halide-poor and halide-rich conditions for NCs. Reprinted with permission from ref 37. Copyright 2017 American Chemical Society.

DOI: 10.1021/acs.jpclett.9b00689
J. Phys. Chem. Lett. 2019, 10, 2629−2640

Halide-rich conditions were used to prepare $CsPbBr_3$ NCs (Figure 1c). Passivating defects with the lowest formation energies, like halide vacancies, during NC synthesis under halide-rich conditions, by replacing $PbBr_2$ with PbO and NH_4Br, was found to be beneficial for obtaining NCs with high PLQYs and stability.[37] LED devices prepared with NCs synthesized under halide-rich conditions showcased better parameters than devices containing NCs synthesized under halide-poor conditions. An LED containing $CsPbBr_3$ NCs in a 1:4 Pb:Br proportion with a current efficiency of 3.1 cd A^{-1} showed a distinctly increased maximum luminance of 12090 cd m^{-2} and an EQE of 1.194%.

The synthesis of $CsPbX_3$ NCs by the hot-injection method requires a compromise regarding the choice of surrounding ligands. On the one hand, these long-chain, insulating ligands create an unfavorable electronic energy barrier and impede electronic coupling between particles, which normally exhibit exceptionally tunable optical properties and high PLQYs; that barrier limits charge transport in devices. On the other hand, such ligands are required for the processing and defect passivation of the NCs. Striking that balance points to the two most important challenges facing the fabrication of efficient LEDs: the replacement of the long ligands with shorter ones without influencing the light-emitting properties and stability; and the discovery of efficient defect-passivating ligands.

Striking that balance points to the two most important challenges facing the fabrication of efficient LEDs: the replacement of the long ligands with shorter ones without influencing the light-emitting properties and stability; and the discovery of efficient defect-passivating ligands.

To overcome these limitations, Pan et al. proposed a postsynthesis passivation method using bidentate ligands (2,2′-iminodibenzoic acid (IDA)) (Figure 2a).[38] Once passivated, the $CsPbI_3$ NCs demonstrated favorable properties: narrow red photoluminescence, near-unity quantum yield, and significantly enhanced stability. Additionally, the NCs prepared with this passivation strategy allowed the fabrication of red color LEDs with an EQE of 5.02% and a reasonable luminance of 748 cd/m^2. The passivated NCs also exhibited substantially improved environmental stability. The NCs with IDA treatment showed better stability and maintained 90% of their PLQY even after 15 days.

With the strong coordination of the P═O group, Wu et al. reported that trioctylphosphine oxide (TOPO) can be a strong capping ligand for inorganic halide perovskite NCs.[39] They demonstrated that $CsPbBr_3$ NC's exhibited greatly improved performance after TOPO treatment. Similarly, Liu et al. achieved a high PLQY of 100% in $CsPbI_3$ NCs. Their approach was to incorporate the trioctylphosphine−PbI_2 (TOP−PbI_2) as a precursor; the stability of the ensuing $CsPbI_3$ NCs was dramatically improved. Octylphosphonic acid (OPA) could also be applied to exchange the capping ligands (OA/OLA) adsorbed on the perovskite NCs during synthesis. Capping $CsPbX_3$ NCs with OPA preserved the particles' high PLQY (>90%) and showed high stability against the purification processes. A green LED based on OPA-$CsPbX_3$ showed an EQE and a current efficiency of 6.5% and 18.13 cd A^{-1}, respectively.[40]

Peptides, with amino and carboxylic functional groups, represent another effective approach for defect passivation (Figure 2b).[41] The synergy between the two groups allows for the generation of ammonium moieties, $R-NH_3^+$. $CH_3NH_3PbBr_3$ as well as $CsPbBr_3$ PNCs have been synthesized through this strategy, using peptides of varying length. Moreover, by adjusting the peptide concentration, peptide-based PNCs with a size variation of ∼3.9−8.6 nm can also be prepared.

Halide ion pair [didodecyldimethylammonium bromide (DDAB)] passivation was reported by Bakr et al. for $CsPbX_3$ NCs, which promoted carrier transport and enabled efficient LEDs (Figure 2c).[42,43] Only a ligand-exchange strategy involving the desorption of protonated oleyamine (OAm) as an intermediate step afforded such films; a direct, more conventional ligand-exchange approach would cause degradation of all-organic NCs. The novel ligand-exchange strategy yielded green LEDs with a luminance and a high EQE of 330 cdm^{-2} and 3.0%, respectively. Furthermore, the application of a similar treatment to fabricate blue LEDs resulted in a EQE of 1.9% and luminance of 35 cdm^{-2}.

As reported by Imran et al., the use of secondary amines can also yield uniform $CsPbBr_3$ nanocubes.[44] The authors' novel colloidal synthesis method afforded only cube-shaped NCs independently of alkyl chain length, oleic acid concentration, or reaction temperature. The authors attribute the uniform and phase pure NCs to interference caused by the secondary amines—specifically, their inability to settle into a favorable configuration on NC surfaces.

Vickers et al. reported short conductive aromatic ligands such as benzylamine (BZA) and benzoic acid (BA). In turn, it facilitated charge transport between quantum dots (QDs).[45] The BZA-BA-$MAPbBr_3$ QDs were significantly stable, showed a maximum PLQY of 86%, and—according to electrochemical and photovoltage spectroscopy and transient photocurrent—outperformed PQDs with insulating ligands with respect to carrier lifetime and charge extraction efficiency.

Krieg et al. developed a novel ligand-capping method involving commercially available zwitterionic molecule, 3-(*N*,*N*-dimethyloctadecylammonio)propanesulfonate, which allowed for much stronger adhesion to NC surfaces via the chelate effect (Figure 2d).[46] The authors designed the strategy to improve the processing and colloidal stability and structural integrity. In addition to affording appreciably higher yields of NCs, ligands of this type enabled high stability against washing.

The use of amine-based passivating materials (APMs) provides notable benefits, such as defect passivation by bonding between the undercoordinated Pb and nitrogen (Figure 2e). The authors indicated that APMs allowed for enhanced PL intensity, suppressed PL blinking, and a long PL lifetime, thereby enhancing device performance with an EQE of 6.2%. Confocal microscopy revealed the suppressing of PL quenching in perovskite semiconductors due to the passivation effect from ethylenediamine (EDA) treatment.[47]

Anionic X-type ligands also impart favorable properties. Such ligands enable trap-free band gaps through replacing surface halide vacancy sites; the result is the promotion of Pb 6p levels to those where they no longer manifest between band gap. X-type ligands passivate undercoordinated lead atoms, raising the

DOI: 10.1021/acs.jpclett.9b00689
J. Phys. Chem. Lett. 2019, 10, 2629−2640

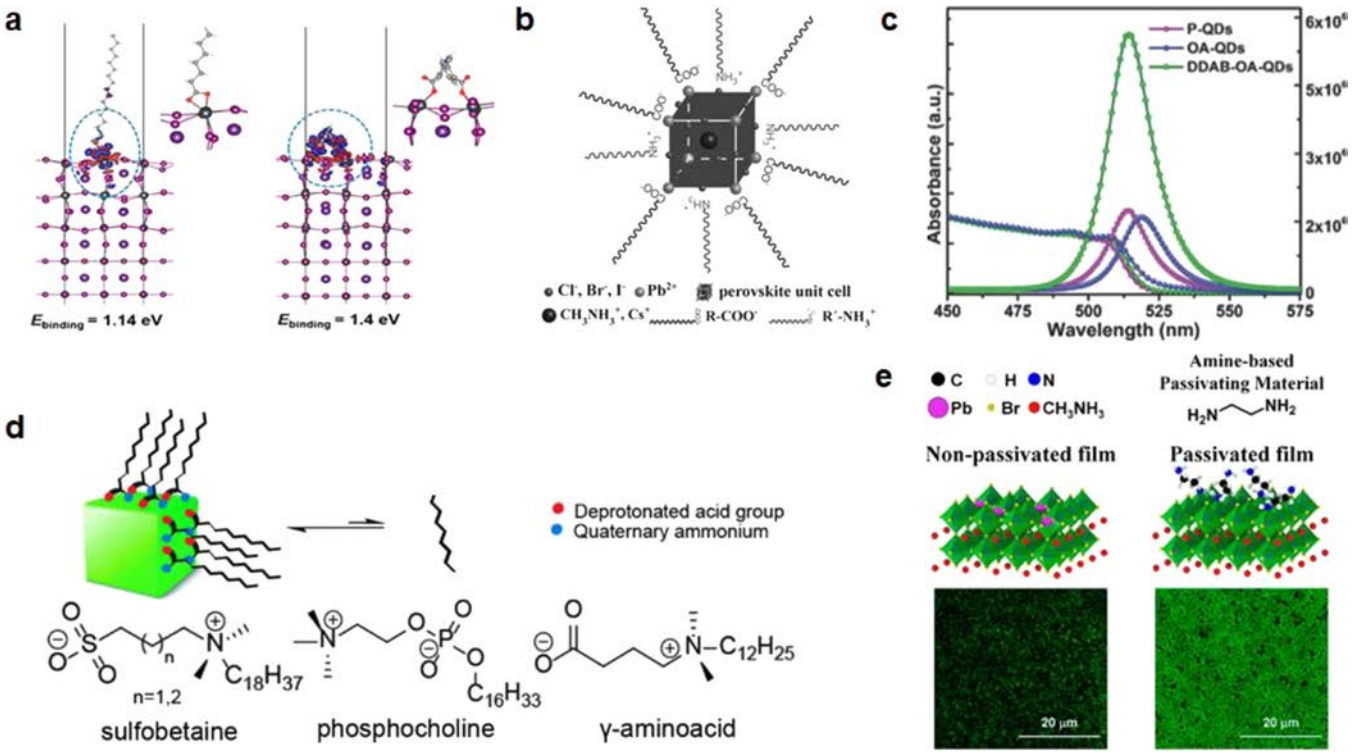

Figure 2. (a) Redistributions of surface charge for optimized PbI_2-rich $CsPbI_3$ surfaces with oleic acid (OA) and IDA bidentate ligand modification. Reprinted with permission from ref 38. Copyright 2018 American Chemical Society. (b) Schematic diagram illustrating the surface passivation mechanism using peptides. Adapted from ref 41. Copyright 2017 Wiley-VCH. (c) Absorption and PL spectrum of purified QDs (P-QDs), OA-QDs, and DDAB-OA-QDs. Adapted from ref 42. Copyright 2016 Wiley-VCH. (d) Schematic diagram illustrating zwitterionic capping ligands. Adapted from ref 46. Copyright 2018 American Chemical Society. (e) Confocal PL images for $MAPbBr_3$ films with and without amine-based passivating materials. Reprinted with permission from ref 47. Copyright 2017 American Chemical Society.

absolute QYs to near unity, which indicates full trap passivation.[48]

A summary of the ligands applied for surface passivation of perovskite NCs is shown in Figure 3.

Doping is widely applied to tune the emission peaks of perovskite NCs because of energy transfer between hosts and dopants[49−55] Both isovalent (divalent) and heterovalent (monovalent and trivalent) metal ions have been reported for doping of perovskite NCs.[55−60] In addition to tuning the emission peak, doping is also an effective strategy for reducing defects in perovskite NCs without influencing their size or crystal structure. Here, we focus only on cases related to the defect chemistry relevant to metal or rare-earth doping. Doping can be realized either by growth doping, in which metal ions are directly introduced into the precursor, or by diffusion doping, usually via post-treatment because of fast ion exchange with perovskite NCs.[51] The doped metal ions are distributed either in the lattice, which could induce changes in the lattice constant, or on the surfaces of NCs. Numerous studies have reported positive roles of metal-ion or rare-earth doping in suppressing crystallographic defects, including point defects (vacancies) or structure disorder (distortion of the $[PbX_6]$ octahedra), in perovskite NCs.

In addition to tuning the emission peak, doping is also an effective strategy for reducing defects in perovskite NCs without influencing their size or crystal structure.

Despite fine optimization of synthesis conditions, the imperfect assembly of constituents during a reaction still exists and it is the main reason for lower PLQY of $CsPbCl_3$ NCs. These imperfections in crystals, likely due to vacancies and/or surface excess Pb and/or distorted $[PbX_6]$ octahedra. Yong et al. reported the effects of incorporating a small amount of divalent foreign ions, Ni^{2+} in their case, into the $CsPbX_3$ matrix. In particular, the improved order of the lattice arises from the increased defect formation energy after introducing the dopant. The reduction of nonradiative recombination rate from 378.29 to 1.90 μs^{-1} (optimized condition) was observed, which indicates the decreased population of nonradiative recombination centers (Figure 4a,b). A maximum PLQY of 96.5% was achieved by Ni^{2+} doping strategy. From the density functional theory (DFT) calculations, it is proved that the Cl vacancy creates a gap state in pristine $CsPbCl_3$ and no defect states for doped $CsPbCl_3$ (Figure 4c,d).[61]

Bi et al. reported the favorable effects of doping smaller Cu^{2+} ions into $CsPb(Br/Cl)_3$: lattice contraction and elimination of halide vacancies. The authors reported that Cu^{2+} also led to improvements of light emitting and stability of NCs.[62]

Divalent metal ion Zn^{2+} was also proven effective both in $CsPbBr_3$ and $CsPbI_3$ NCs for defect passivation. $ZnBr_2$-doped $CsPbBr_3$ NCs showed a PLQY of 78%, which was dramatically higher than pristine $CsPbBr_3$ NCs with PLQY of 54% without a shift in the emission peak. Two possible mechanisms were proposed to explain the defect passivation effect induced by Zn^{2+}

DOI: 10.1021/acs.jpclett.9b00689
J. Phys. Chem. Lett. 2019, 10, 2629−2640

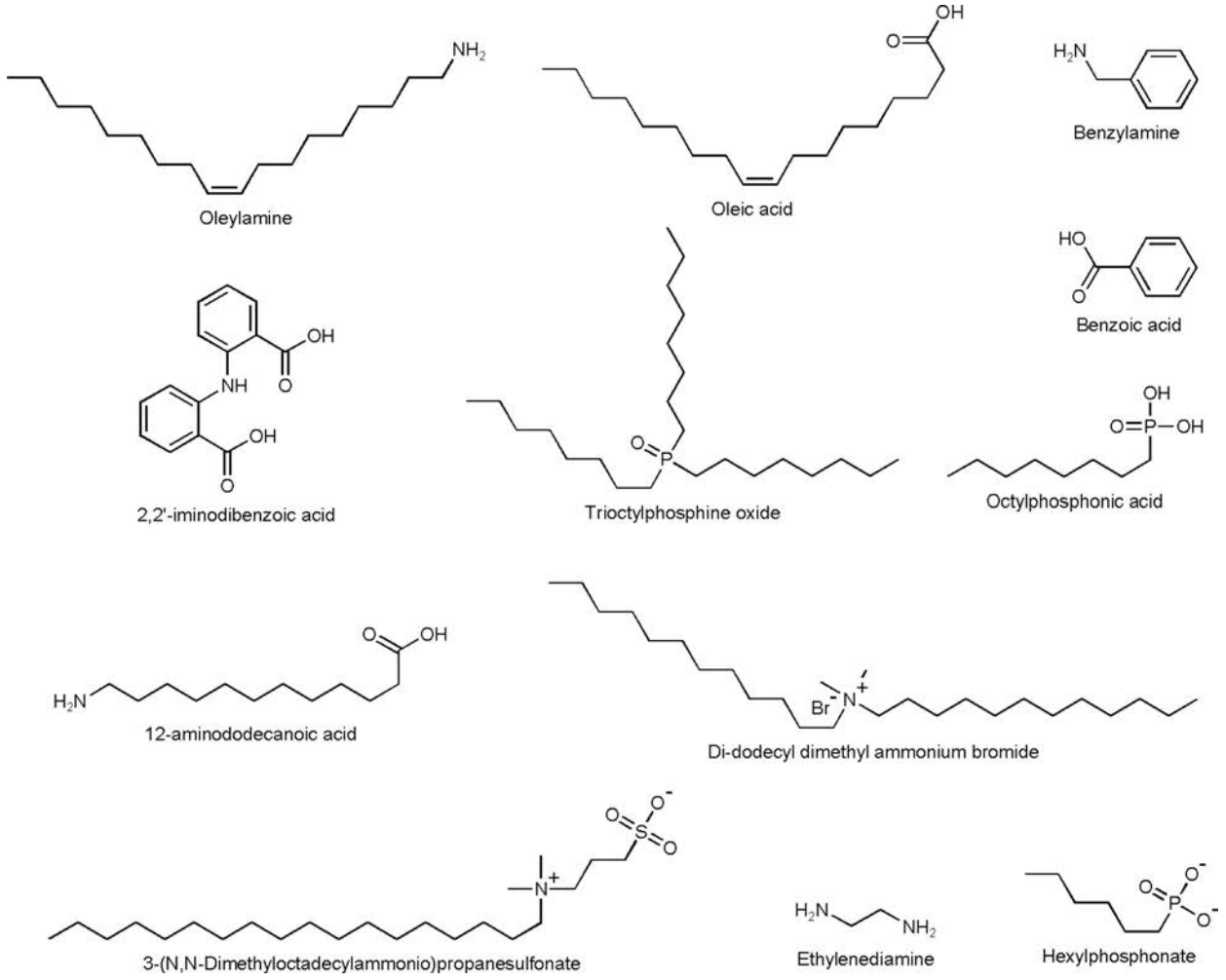

Figure 3. Brief summary of the ligands applied for surface passivation of perovskite NCs.

doping: (1) the favorable formation energies attained by the introduction of $ZnBr_2$ into reaction solutions lead to the coverage of $CsPbBr_3$ NC surfaces with $PbBr_2$ adlayer, and (2) introducing $ZnBr_2$ into the reaction may give rise to lead bromide-rich conditions. Various other metal bromides ($CuBr_2$ and $InBr_3$) have also shown efficacy.[63]

Defect passivation enabled by alloying Zn^{2+} into $CsPbI_3$ NCs has likewise been demonstrated. Defect densities of 1.26×10^{17} and 1.75×10^{16} cm^{-3} were estimated for pristine $CsPbI_3$ and for Zn and Pb alloyed films ($CsPb_{0.64}Zn_{0.36}I_3$), respectively, by the space-charge-limited current (SCLC) method. Those figures represent a substantial decrease of nearly 1 order of magnitude upon incorporating Zn^{2+}. The larger value of the atomic ratio of I/(Zn + Pb) led to the transition of the surface elemental environment from one rich in lead to one rich in iodine upon introducing Zn^{2+}. Moreover, the alloying also improved the stability by lattice contraction, and the α-phase of the NCs could remain stable in air for 70 days. A large luminance (2202 cd m^{-2}), low turn-on voltage (2 V), and a high EQE (15.1%) were achieved (Figure 4e).[64]

Navendu et al. reported doping of Cd^{2+} into $CsPbCl_3$ NCs by $CdCl_2$ post-treatment. The PLQY of $CsPbCl_3$ NCs was increased to near unity (96 ± 2%) with the $CdCl_2$ post-treatment. The decreasing of defect state density after $CdCl_2$ post-treatment was proved by time-resolved photoluminescence lifetime (TRPL) and ultrafast transient absorption (TAS).[65,66]

Digging deeper, an excellent example illustrating the mechanism of small iso-valent metal-ion (Zn^{2+}, Cd^{2+}, etc.) doping is the reduction of the defect population of the polycrystalline thin films by such doping (Figure 4f). The size mismatch results in the lattice strain. This mismatch of ionic size between the sizes of the lead halide cage and A cation results in strains (cage distortions and BX_6 octahedron tilting in the ABX_3 perovskite structure). To release the strain in $FAPbI_3$, point defect formation is favorable. The incorporation of small isovalent metal ions creates an alternative pathway for relaxing lattice strain (other than vacancy formation) in perovskites, thereby preventing defect formation. Saidaminov et al. used Cd^{2+}, which is isovalent to Pb^{2+} but has a smaller ionic radius, for further relaxation of lattice strain without introducing traps.[36]

Defects in crystalline semiconductors can be classified into two categories: lattice interruptions (crystallographic defects) or foreign atoms (impurities).[64] Thus, heterovalent dopants—as foreign atoms—could create impurity levels, either deep or shallow traps.[67,68] However, this approach could be beneficial for promoting light emission when the doping of heterovalent metal ions only induces shallow states. Doping with heterovalent Ce^{3+} ions has been reported to not introduce trap states, resulting from the similar ionic radii and the formation of a higher conduction band energy level with bromine relative to that formed with the Pb^{2+} cation.[69] When doping 2.88% Ce^{3+}

DOI: 10.1021/acs.jpclett.9b00689
J. Phys. Chem. Lett. 2019, 10, 2629−2640

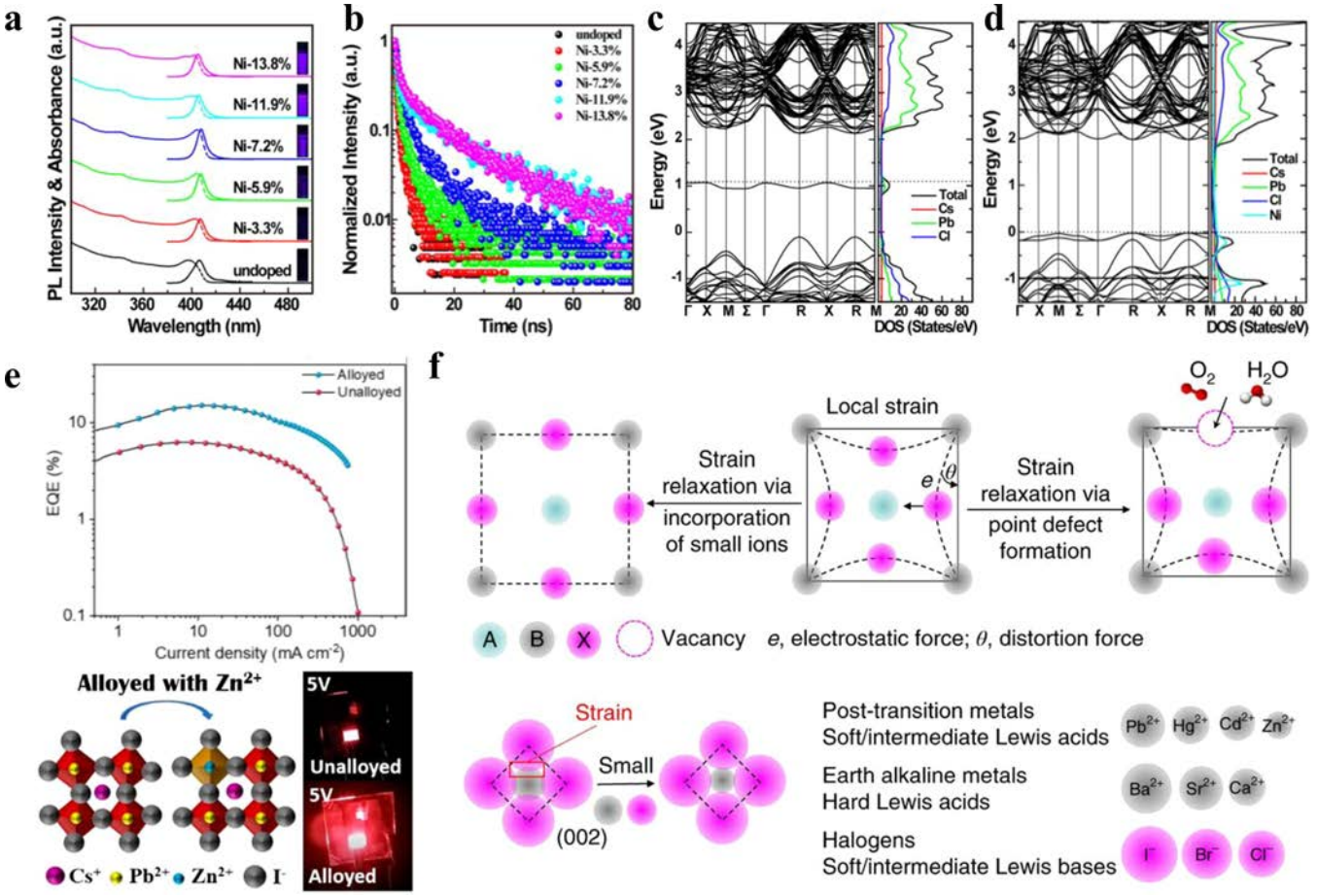

Figure 4. (a) PL and absorption for $CsPbCl_3$ NCs with different Ni^{2+} concentration. (b) PL decay for $CsPbCl_3$ NCs with different Ni^{2+} concentration. (c) and (d) Density of states (DOS) and energy band configuration for pristine and doped $CsPbCl_3$, respectively. Reprinted with permission from ref 61. Copyright 2018 American Chemical Society. (e) EQEs for $CsPbI_3$ and alloyed $CsPb_{0.64}Zn_{0.36}I_3$ NCs LEDs and photographs of the respective working LEDs. Reprinted with permission from ref 64. Copyright 2019 American Chemical Society. (f) Schematic illustrating local strain. Reprinted with permission from ref 36. Copyright 2018 Nature Publishing Group.

into $CsPbBr_3$ NCs, PLQY of $CsPbBr_3$ NCs achieved 89%, compared with 41% for undoped NCs.

Recently, Jun et al. further uncovered the mechanism of heterovalent doping in $CsPbBr_3$, namely, by high-level DFT.[70] The results showed that PL quenching was induced by the deep trap states when Bi^{3+} was used as dopant. However, when applying Ce^{3+} as dopant, the disorder of host NC was reduced, and the edge states were enriched by Ce_{Pb} antisite, and thereafter higher PL was achieved.

Unlike doping strategy, which mainly aims to reduce structure ($[PbX_6]$ octahedra) disorder and increase the defect formation energy, the elemental compensation strategy aims to annihilate surface vacancies by donating the elements required to fill these vacancy sites. Metal halides could provide both metal ions and halides for the surface elemental compensation of perovskite NCs. The post-treatment strategy involving the direct addition of $PbBr_2$ to a pristine solution of $CsPbBr_3$ NCs induces excess bromide and stronger binding of ligand, both of which can enhance the PL.[71] The post-treatment by ZnX_2 was also reported. After post-treatment, halogen vacancies, which are abundant on QDs of this type were completely removed, as verified by high-resolution transmission electron microscopy (HRTEM), resulting in enhanced stability and PL (Figure 5a,b). The ZnX_2/hexane solution post-treatment is universal to several compositions, including $CsPbCl_3$, $CsPbBr_3$, and $CsPbI_3$.[72]

The small monovalent cation potassium (K^+) has proven to be a highly effective passivator in polycrystalline perovskite films. K^+ is effective in passivating the surface of perovskite grains. Abdi-Jalebi et al. introduced excess iodide by incorporating potassium iodide into perovskite precursor and thereby compensated for halide vacancies. The optimized perovskite films with K^+ reached a very high PLQE of 66% (Figure 5c).[73] As illustrated in Figure 5d, the filling of these vacancies with excess halides passivates the nonradiative recombination centers. The migration of halide was also inhibited by excess halides. However, K^+ passivation has not yet been demonstrated in NCs.

YCl_3, a trivalent metal chloride salt, was used for the dual-surface passivation of $CsPbCl_3$ NCs. The dual-surface passivation was enabled by that Y^{3+} bonded to uncoordinated Pb atoms, and the Cl reach surface, which was proved by X-ray photoelectron spectroscopy (XPS) and substituting Y-acetate salt for YCl_3 (Figure 5e,f). DFT results indicate that Y^{3+} and Cl^- ions cannot create the mip-gap states but enrich conduction band (CB) states. This dual-passivation strategy markedly increased the PLQY from 1 to 60%.[74] Defect passivation in $CsPbI_3$ NCs is also realized by the Cl^- anions carried by $SrCl_2$. Surface Cl^- ion passivation was shown to enhance the PLQY (by up to 84%) of $CsPbI_3$ NCs.[75]

The thiocyanate (SCN^-) anion can be incorporated into the perovskite lattice. Mixed-anion perovskites (CH_3NH_3Pb-

DOI: 10.1021/acs.jpclett.9b00689
J. Phys. Chem. Lett. 2019, 10, 2629−2640

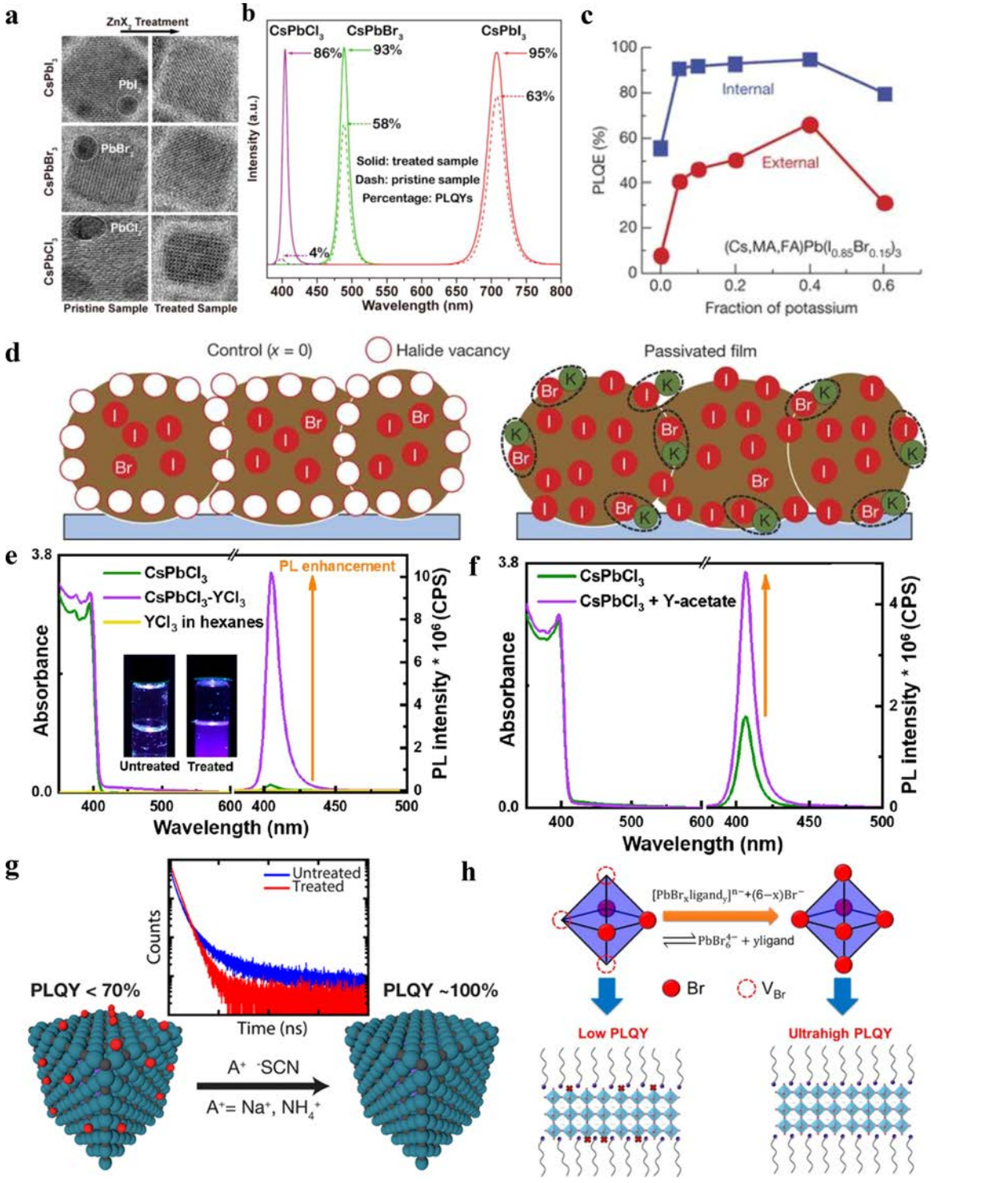

Figure 5. (a) HRTEM images of pristine and $CsPbX_3$ NCs with ZnX_2 treatment. (b) PL of pristine and $CsPbX_3$ NCs with ZnX_2 treatment. Reprinted with permission from ref 72. Copyright 2018 American Chemical Society. (c) PLQE of passivated films by changing of potassium ratio. (d) Schematic of K passivation of halide vacancy when there is excess halide. Reprinted with permission from ref 73. Copyright 2018 Nature Publishing Group. (e) PL and absorption spectrum for pristine and treated $CsPbCl_3$ NCs. (f) PL and absorption spectra for pristine and Y $(CH_3CO_2)_3$-treated NCs. Reprinted with permission from ref 74. Copyright 2018 American Chemical Society. (g) TRPLs of pristine $CsPbBr_3$ NCs and treated-$CsPbBr_3$ by ammonium thiocyanate and schematic of interaction between thiocyanate and $CsPbBr_3$ NC surface defect sites. Adapted with permission from ref 82. Copyright 2017 American Chemical Society. (h) Schematic of $PbBr_6^{4-}$ octahedra with and without V_{Br} and corresponding influence on PLQY. Reprinted with permission from ref 85. Copyright 2018 American Chemical Society.

$(SCN)_xI_{3-x}$) has been shown to benefit structure stability against moisture.[76−78] Moreover, a $CH_3NH_3Pb(SCN)_xI_{3-x}$ polycrystalline thin film was reported to exhibit large crystal sizes with decreased trap states.[79−81] The SCN^- ion also plays positive roles in suppressing defects in perovskite NCs. Koscher et al. applied SCN^- from either NH_4SCN or NaSCN to enhance PLQY of $CsPbBr_3$ NCs (Figure 5g). This treatment effectively removes excess Pb from the surface, thereby removing trap

DOI: 10.1021/acs.jpclett.9b00689
J. Phys. Chem. Lett. 2019, 10, 2629−2640

states induced by excess lead on the surface of NCs and transforming the NCs into near-unity green emitters.[82]

Blue-emitting perovskite NCs have lower PLQYs than do green- and red-emitting NCs because of different defect chemistry and undeveloped passivation stratey.[83,84] Blue emitting $CsPbBr_3$ nanoplatelets (NPLs) with 96% PLQY was realized by $PbBr_6^{4-}$ octahedron passivation.[85] HBr aqueous solution was introduced into the reaction and an excess of Br^- environment was induced, thereby driving ionic equilibrium to construct perfect $PbBr_6^{4-}$ octahedra (Figure 5h). The reduction of bromide vacancies was indicated by a smaller Urbach energy and a longer transient absorption delay. NPLs based blue LEDs attained a high EQE of 0.124%. Cl passivation induced by metal chlorides and ammonium chloride salts was applied to enhance the PLQY of blue-emitting $CsPbCl_3$ NCs.[84] Blue emitting lead-free $MA_3Bi_2Br_9$ QDs with PLQY of 54.1% was achieved by also Cl passivation. Cl^- anions, as passivation agents, are constrained to the NCs' surface and dramatically reduce the trap states and boost the PLQY.[83]

In a core−shell NC, the shell provides a physical barrier that moderates the sensitivity of the optical properties of the core to environmental variation near the NC surface when exposed to oxygen or water molecules. Moreover, the shell effectively passivates surface trap states, resulting in a strongly enhanced PLQY.[86] Therefore, construction of a core−shell structure is highly attractive for improving both the PLQY and stability of perovskite NCs.

Construction of a core−shell structure is highly attractive for improving both the PLQY and stability of perovskite NCs.

The most efficient perovskite green LED reported to date, with a EQE over 20%, is based on a $CsPbBr_3$/MABr quasi-core−shell structure, which represents a good example that can be transferred to NCs (Figure 6a,b).[10] The $CsPbBr_3$/MABr quasi-core−shell was constructed by covering a presynthesized $CsPbBr_3$ film with a MABr layer. A shell of MABr is formed between the grain boundaries of $CsPbBr_3$, and surface of $CsPbBr_3$, forming the quasi-core−shell structure. Results showed that the MABr shell reduced the number of defects in $CsPbBr_3$/MABr perovskite films.

NC/silica composites were also synthesized and showed high PLQY and extremely high stability in air (Figure 6c). (3-Aminopropyl)triethoxysilane (APTES) could undergo hydrolysis induced by trace water vapor in air, and a silica matrix subsequently formed slowly on perovskite NCs. The amino group in APTES could effectively passivate the NC surface to maintain the original high PLQY.[87]

A Mn^{2+}-doped $CsPbCl_3$ NC/undoped $CsPbCl_3$ core−shell structure was adopted to protect the surface dopant ions (Mn^{2+}) and enhance the dopant light emission (Figure 6d).[88] To grow a $CsPbCl_3$-shell layer, the Mn^{2+}-doped $CsPbCl_3$ NCs were redispersed in toluene. Luminescent ions near the surface are well-known to experience faster decay than those farther away due to energy transfer to surface defects. The lifetime of Mn^{2+} emission can be appreciably prolonged, as confirmed by a reduced quenching effect from surface defect sites.

Despite the remarkable success and progress achieved, many challenges remain to be addressed concerning passivation strategies and the understanding of defect chemistry for further improving perovskite NC light-emitting devices. We conclude by listing several crucial challenges for further research.

(1) Ligand detachment and self-assembly. The ligands of NCs suspended in solution are in a dynamic equilibrium between the crystal NCs surface and the solution. Over time, ligands can detach from the surface of the NCs and scavenge lead or halide ions on the surface of QDs, which creates more vacancies. After ligand detachment, the NCs are easily aggregated and regrow due to the reduced barrier from the surface ligands and easily moving ions of perovskite NCs.[89]

(2) Defect species in NCs and full passivation of different types of defects. The types of defects that actually exist in NC's of various composition and the corresponding population should be elucidated for targeted passivation.

(3) Composition-dependent defect chemistry. Changing composition can dramatically vary the defect chemistry of perovskite NCs and represents a primary reason for the inferior performance of blue-emitting perovskites compared with the performance of green- and red-emitting perovskites. For blue-emitting mixed-halide perovskites ($CsPbBr_xCl_{3-x}$), Cl vacancies (V_{Cl}) are deep traps and are highly energetically favorable. An effective defect passivation strategy for blue-emitting mixed-halide perovskites remains to be established.

(4) Insightful understanding of passivation mechanism. A series of strategies have been proposed to realize high-efficiency PL from halide perovskite NCs. However, in many cases the detailed investigations of NCs structures remain missing. Systematic structural and photophysical characterizations coupled with first-principles calculations could deepen the understanding of underlying mechanisms for the passivation methods used. For instance, doping engineering can be used for optimization of the performance of perovskite NCs, but the critical factors governing the doping efficiency and the exact distribution of dopants in NCs remain elusive in most doped NCs.[90] Similarly, for postsynthetic treatment, it requires a deeper understanding of the role of metal cations that play in the removal of defects.

(5) Core−shell perovskite NCs. At present, construction of perovskite core−shell NCs remains a significant challenge. There are numerous perovskite compositions, the band gaps of which can be easily tuned. Thus, numerous perovskite−perovskite core−shell structures can be constructed, and new interfacial chemistry and physics could be further explored. Many successfully fabricated heterojunction core−shell structures, such as CdSe/CdS, CdSe/CdZnS, and InP/ZnS core−shell NCs, have been well studied. Other semiconductors with a small lattice mismatch with perovskites should be explored to passivate surface trap states and encapsulate the environmentally sensitive perovskite NCs inside.

In summary, tremendous progress has been made in eliminating defects in perovskite NCs for fabricating efficient light-emitting devices. This Perspective discussed the strategies established for defect reduction and examined the potential mechanisms that underlie these strategies. Numerous methods for reducing the defect states of NCs have been developed, including advanced NC syntheses, new surface-capping strategies, doping with metal ions and rare earths, engineering elemental compensation, and the translation of core−shell

DOI: 10.1021/acs.jpclett.9b00689
J. Phys. Chem. Lett. 2019, 10, 2629−2640

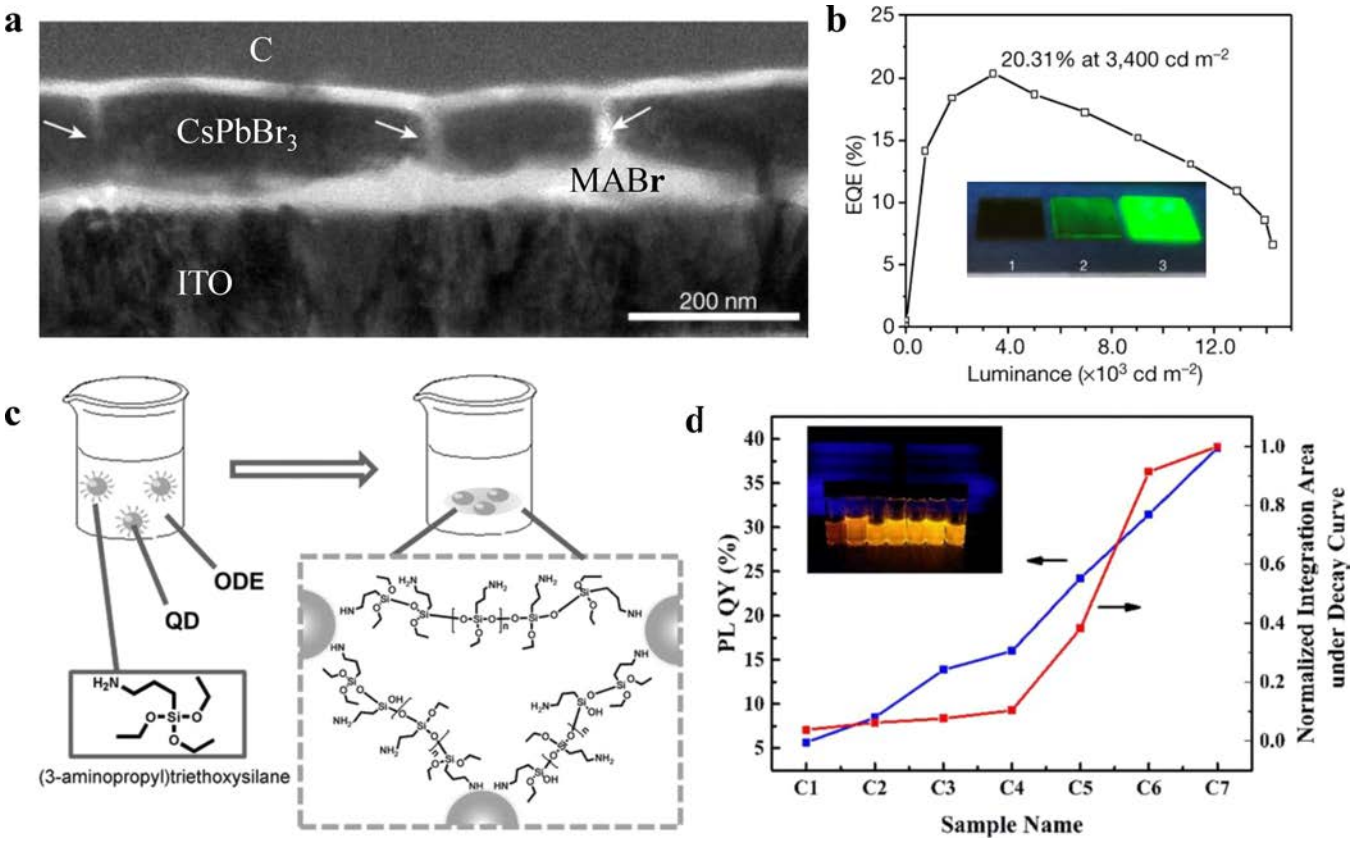

Figure 6. (a) Cross-sectional TEM image of a quasi-core−shell $CsPbBr_3$/MABr structure. Reprinted with permission from ref 10. Copyright 2018 Nature Publishing Group. (b) EQE characteristics of quasi-core−shell $CsPbBr_3$/MABr LEDs. Inset: photographs of single-layer $CsPbBr_3$, bilayer $CsPbBr_3$/MABr, and quasi-core−shell $CsPbBr_3$/MABr perovskite films under UV light. Reprinted with permission from ref 10. Copyright 2018 Nature Publishing Group. (c) Schematic of synthesis of QD/silica composites. Adapted from ref 87. Copyright 2016 Wiley-VCH. (d) Effect of isocrystalline core−shell on PLQY and integrated area under the Mn^{2+} luminescence decay curves. Samples C1 to C7 are Mn^{2+}/$CsPbCl_3$ without a $CsPbCl_3$ shell to Mn^{2+}/$CsPbCl_3$ with the thickest $CsPbCl_3$ shell from left to right. Reprinted with permission from ref 88. Copyright 2017 American Chemical Society.

This Perspective discussed the strategies established for defect reduction and examined the potential mechanisms that underlie these strategies.

heterostructures. Nevertheless, various challenges await to be addressed, and further research efforts are needed to solve these problems.

AUTHOR INFORMATION

Corresponding Authors

*E.H.S. (ted.sargent@utoronto.ca).
*O.M.B. (osman.bakr@kaust.edu.sa).

ORCID

Yi Hou: 0000-0002-1532-816X
Hong-Tao Sun: 0000-0002-0003-7941
Omar F. Mohammed: 0000-0001-8500-1130
Edward H. Sargent: 0000-0003-0396-6495
Osman M. Bakr: 0000-0002-3428-1002

Author Contributions

‖These authors contributed equally.

Notes

The authors declare no competing financial interest.

ACKNOWLEDGMENTS

This work was supported by King Abdullah University of Science and Technology (KAUST) baseline funding and Office of Sponsored Research (OSR) under award No. OSR-2017-CRG-3380.

REFERENCES

(1) Xiao, Z.; Kerner, R. A.; Zhao, L.; Tran, N. L.; Lee, K. M.; Koh, T.-W.; Scholes, G. D.; Rand, B. P. Efficient Perovskite Light-Emitting Diodes Featuring Nanometre-sized Crystallites. *Nat. Photonics* **2017**, *11*, 108.

(2) Akkerman, Q. A.; Rainò, G.; Kovalenko, M. V.; Manna, L. Genesis, Challenges and Opportunities for Colloidal Lead Halide Perovskite Nanocrystals. *Nat. Mater.* **2018**, *17*, 394−405.

(3) Chen, Q.; Wu, J.; Ou, X.; Huang, B.; Almutlaq, J.; Zhumekenov, A. A.; Guan, X.; Han, S.; Liang, L.; Yi, Z.; et al. All-Inorganic Perovskite Nanocrystal Scintillators. *Nature* **2018**, *561*, 88−93.

(4) Zhang, L.; Yang, X.; Jiang, Q.; Wang, P.; Yin, Z.; Zhang, X.; Tan, H.; Yang, Y.; Wei, M.; Sutherland, B. R.; et al. Ultra-Bright and Highly Efficient Inorganic Based Perovskite Light-Emitting Diodes. *Nat. Commun.* **2017**, *8*, 15640.

(5) Swarnkar, A.; Marshall, A. R.; Sanehira, E. M.; Chernomordik, B. D.; Moore, D. T.; Christians, J. A.; Chakrabarti, T.; Luther, J. M. Quantum Dot−Induced Phase Stabilization of α-$CsPbI_3$ Perovskite for High-Efficiency Photovoltaics. *Science* **2016**, *354*, 92−95.

DOI: 10.1021/acs.jpclett.9b00689
J. Phys. Chem. Lett. 2019, 10, 2629−2640

(6) Wang, N.; Cheng, L.; Ge, R.; Zhang, S.; Miao, Y.; Zou, W.; Yi, C.; Sun, Y.; Cao, Y.; Yang, R.; et al. Perovskite Light-Emitting Diodes Based on Solution-Processed Self-Organized Multiple Quantum Wells. *Nat. Photonics* **2016**, *10*, 699.
(7) Song, J.; Li, J.; Li, X.; Xu, L.; Dong, Y.; Zeng, H. Quantum Dot Light-Emitting Diodes Based on Inorganic Perovskite Cesium Lead Halides ($CsPbX_3$). *Adv. Mater.* **2015**, *27*, 7162−7167.
(8) Zhang, X.; Liu, H.; Wang, W.; Zhang, J.; Xu, B.; Karen, K. L.; Zheng, Y.; Liu, S.; Chen, S.; Wang, K.; et al. Hybrid Perovskite Light-Emitting Diodes Based on Perovskite Nanocrystals with Organic−Inorganic Mixed Cations. *Adv. Mater.* **2017**, *29*, 1606405.
(9) Bodnarchuk, M. I.; Boehme, S. C.; ten Brinck, S.; Bernasconi, C.; Shynkarenko, Y.; Krieg, F.; Widmer, R.; Aeschlimann, B.; Günther, D.; Kovalenko, M. V. Rationalizing and Controlling the Surface Structure and Electronic Passivation of Cesium Lead Halide Nanocrystals. *ACS Energy Lett.* **2019**, *4*, 63−74.
(10) Lin, K.; Xing, J.; Quan, L. N.; de Arquer, F. P. G.; Gong, X.; Lu, J.; Xie, L.; Zhao, W.; Zhang, D.; Yan, C.; et al. Perovskite Light-Emitting Diodes with External Quantum Efficiency Exceeding 20 Per Cent. *Nature* **2018**, *562*, 245−248.
(11) Chiba, T.; Hayashi, Y.; Ebe, H.; Hoshi, K.; Sato, J.; Sato, S.; Pu, Y.-J.; Ohisa, S.; Kido, J. Anion-Exchange Red Perovskite Quantum Dots with Ammonium Iodine Salts for Highly Efficient Light-Emitting Devices. *Nat. Photonics* **2018**, *12*, 681−687.
(12) Cao, Y.; Wang, N.; Tian, H.; Guo, J.; Wei, Y.; Chen, H.; Miao, Y.; Zou, W.; Pan, K.; He, Y.; et al. Perovskite Light-Emitting Diodes Based on Spontaneously Formed Submicrometre-Scale Structures. *Nature* **2018**, *562*, 249−253.
(13) Zhang, Y.; Sun, R.; Ou, X.; Fu, K.; Chen, Q.; Ding, Y.; Xu, L.-J.; Liu, L.; Han, Y.; Malko, A. V.; et al. Metal Halide Perovskite Nanosheet for X-ray High-Resolution Scintillation Imaging Screens. *ACS Nano* **2019**, *13*, 2520−2525.
(14) Huang, H.; Polavarapu, L.; Sichert, J. A.; Susha, A. S.; Urban, A. S.; Rogach, A. L. Colloidal Lead Halide Perovskite Nanocrystals: Synthesis, Optical Properties and Applications. *NPG Asia Mater.* **2016**, *8*, e328.
(15) Yuan, M.; Quan, L. N.; Comin, R.; Walters, G.; Sabatini, R.; Voznyy, O.; Hoogland, S.; Zhao, Y.; Beauregard, E. M.; Kanjanaboos, P.; et al. Perovskite Energy Funnels for Efficient Light-Emitting Diodes. *Nat. Nanotechnol.* **2016**, *11*, 872.
(16) Chen, Z.; Zhang, C.; Jiang, X.-F.; Liu, M.; Xia, R.; Shi, T.; Chen, D.; Xue, Q.; Zhao, Y.-J.; Su, S.; et al. High-Performance Color-Tunable Perovskite Light Emitting Devices through Structural Modulation from Bulk to Layered Film. *Adv. Mater.* **2017**, *29*, 1603157.
(17) Bade, S. G. R.; Li, J.; Shan, X.; Ling, Y.; Tian, Y.; Dilbeck, T.; Besara, T.; Geske, T.; Gao, H.; Ma, B.; et al. Fully Printed Halide Perovskite Light-Emitting Diodes with Silver Nanowire Electrodes. *ACS Nano* **2016**, *10*, 1795−1801.
(18) Dong, Y.; Zhao, Y.; Zhang, S.; Dai, Y.; Liu, L.; Li, Y.; Chen, Q. Recent Advances toward Practical Use of Halide Perovskite Nanocrystals. *J. Mater. Chem. A* **2018**, *6*, 21729−21746.
(19) Wang, N.; Liu, W.; Zhang, Q. Perovskite-Based Nanocrystals: Synthesis and Applications beyond Solar Cells. *Small Methods* **2018**, *2*, 1700380.
(20) Tanaka, K.; Kondo, T. Bandgap and Exciton Binding Energies in Lead-Iodide-Based Natural Quantum-Well Crystals. *Sci. Technol. Adv. Mater.* **2003**, *4*, 599−604.
(21) Huang, J.; Yuan, Y.; Shao, Y.; Yan, Y. Understanding the Physical Properties of Hybrid Perovskites for Photovoltaic Applications. *Nat. Rev. Mater.* **2017**, *2*, 17042.
(22) Park, Y.-S.; Guo, S.; Makarov, N. S.; Klimov, V. I. Room Temperature Single-Photon Emission from Individual Perovskite Quantum Dots. *ACS Nano* **2015**, *9*, 10386−10393.
(23) Kim, Y.-H.; Wolf, C.; Kim, Y.-T.; Cho, H.; Kwon, W.; Do, S.; Sadhanala, A.; Park, C. G.; Rhee, S.-W.; Im, S. H.; et al. Highly Efficient Light-Emitting Diodes of Colloidal Metal−Halide Perovskite Nanocrystals beyond Quantum Size. *ACS Nano* **2017**, *11*, 6586−6593.
(24) Swarnkar, A.; Chulliyil, R.; Ravi, V. K.; Irfanullah, M.; Chowdhury, A.; Nag, A. Colloidal CsPbBr3 Perovskite Nanocrystals: Luminescence beyond Traditional Quantum Dots. *Angew. Chem.* **2015**, *127*, 15644−15648.
(25) Sichert, J. A.; Tong, Y.; Mutz, N.; Vollmer, M.; Fischer, S.; Milowska, K. Z.; García Cortadella, R.; Nickel, B.; Cardenas-Daw, C.; Stolarczyk, J. K.; et al. Quantum Size Effect in Organometal Halide Perovskite Nanoplatelets. *Nano Lett.* **2015**, *15*, 6521−6527.
(26) Xiao, Z.; Zhao, L.; Tran, N. L.; Lin, Y. L.; Silver, S. H.; Kerner, R. A.; Yao, N.; Kahn, A.; Scholes, G. D.; Rand, B. P. Mixed-Halide Perovskites with Stabilized Bandgaps. *Nano Lett.* **2017**, *17*, 6863−6869.
(27) Xing, G.; Wu, B.; Wu, X.; Li, M.; Du, B.; Wei, Q.; Guo, J.; Yeow, E. K. L.; Sum, T. C.; Huang, W. Transcending the Slow Bimolecular Recombination in Lead-Halide Perovskites for Electroluminescence. *Nat. Commun.* **2017**, *8*, 14558.
(28) Li, G.; Rivarola, F. W. R.; Davis, N. J. L. K.; Bai, S.; Jellicoe, T. C.; de la Peña, F.; Hou, S.; Ducati, C.; Gao, F.; Friend, R. H.; et al. Highly Efficient Perovskite Nanocrystal Light-Emitting Diodes Enabled by a Universal Crosslinking Method. *Adv. Mater.* **2016**, *28*, 3528−3534.
(29) Protesescu, L.; Yakunin, S.; Bodnarchuk, M. I.; Krieg, F.; Caputo, R.; Hendon, C. H.; Yang, R. X.; Walsh, A.; Kovalenko, M. V. Nanocrystals of Cesium Lead Halide Perovskites ($CsPbX_3$, X = Cl, Br, and I): Novel Optoelectronic Materials Showing Bright Emission with Wide Color Gamut. *Nano Lett.* **2015**, *15*, 3692−3696.
(30) Dong, Y.; Qiao, T.; Kim, D.; Parobek, D.; Rossi, D.; Son, D. H. Precise Control of Quantum Confinement in Cesium Lead Halide Perovskite Quantum Dots via Thermodynamic Equilibrium. *Nano Lett.* **2018**, *18*, 3716−3722.
(31) Dutta, A.; Behera, R. K.; Pal, P.; Baitalik, S.; Pradhan, N. Near-Unity Photoluminescence Quantum Efficiency for All $CsPbX_3$ (X = Cl, Br and I) Perovskite Nanocrystals: A Generic Synthesis Approach. *Angew. Chem., Int. Ed.* **2019**, *58*, 5552.
(32) Dutta, A.; Behera, R. K.; Dutta, S. K.; Das Adhikari, S.; Pradhan, N. Annealing $CsPbX_3$ (X= Cl and Br) Perovskite Nanocrystals at High Reaction Temperatures: Phase Change and Its Prevention. *J. Phys. Chem. Lett.* **2018**, *9*, 6599−6604.
(33) Das Adhikari, S.; Behera, R. K.; Bera, S.; Pradhan, N. Presence of Metal Chloride for Minimizing the Halide Deficiency and Maximizing the Doping Efficiency in Mn(II)-Doped $CsPbCl_3$ Nanocrystals. *J. Phys. Chem. Lett.* **2019**, *10*, 1530−1536.
(34) Tong, Y.; Bladt, E.; Aygüler, M. F.; Manzi, A.; Milowska, K. Z.; Hintermayr, V. A.; Docampo, P.; Bals, S.; Urban, A. S.; Polavarapu, L.; et al. Highly Luminescent Cesium Lead Halide Perovskite Nanocrystals with Tunable Composition and Thickness by Ultrasonication. *Angew. Chem., Int. Ed.* **2016**, *55*, 13887−13892.
(35) Leng, M.; Yang, Y.; Chen, Z.; Gao, W.; Zhang, J.; Niu, G.; Li, D.; Song, H.; Zhang, J.; Jin, S. Surface Passivation of Bismuth-Based Perovskite Variant Quantum Dots to Achieve Efficient Blue Emission. *Nano Lett.* **2018**, *18*, 6076−6083.
(36) Saidaminov, M. I.; Kim, J.; Jain, A.; Quintero-Bermudez, R.; Tan, H.; Long, G.; Tan, F.; Johnston, A.; Zhao, Y.; Voznyy, O.; et al. Suppression of Atomic Vacancies via Incorporation of Isovalent Small Ions to Increase the Stability of Halide Perovskite Solar Cells in Ambient Air. *Nat. Energy* **2018**, *3*, 648−654.
(37) Liu, P.; Chen, W.; Wang, W.; Xu, B.; Wu, D.; Hao, J.; Cao, W.; Fang, F.; Li, Y.; Zeng, Y.; et al. Halide-Rich Synthesized Cesium Lead Bromide Perovskite Nanocrystals for Light-Emitting Diodes with Improved Performance. *Chem. Mater.* **2017**, *29*, 5168−5173.
(38) Pan, J.; Shang, Y.; Yin, J.; De Bastiani, M.; Peng, W.; Dursun, I.; Sinatra, L.; El-Zohry, A. M.; Hedhili, M. N.; Emwas, A.-H. Bidentate Ligand-Passivated $CsPbI_3$ Perovskite Nanocrystals for Stable Near-Unity Photoluminescence Quantum Yield and Efficient Red Light-Emitting Diodes. *J. Am. Chem. Soc.* **2018**, *140*, 562−565.
(39) Liu, F.; Zhang, Y.; Ding, C.; Kobayashi, S.; Izuishi, T.; Nakazawa, N.; Toyoda, T.; Ohta, T.; Hayase, S.; Minemoto, T. Highly Luminescent Phase-Stable $CsPbI_3$ Perovskite Quantum Dots Achieving Near 100% Absolute Photoluminescence Quantum Yield. *ACS Nano* **2017**, *11*, 10373−10383.
(40) Tan, Y.; Zou, Y.; Wu, L.; Huang, Q.; Yang, D.; Chen, M.; Ban, M.; Wu, C.; Wu, T.; Bai, S. Highly Luminescent and Stable Perovskite Nanocrystals with Octylphosphonic Acid as a Ligand for Efficient

DOI: 10.1021/acs.jpclett.9b00689
J. Phys. Chem. Lett. 2019, 10, 2629−2640

Light-Emitting Diodes. *ACS Appl. Mater. Interfaces* **2018**, *10*, 3784−3792.
(41) Luo, B.; Naghadeh, S. B.; Allen, A. L.; Li, X.; Zhang, J. Z. Peptide-Passivated Lead Halide Perovskite Nanocrystals Based on Synergistic Effect between Amino and Carboxylic Functional Groups. *Adv. Funct. Mater.* **2017**, *27*, 1604018.
(42) Pan, J.; Quan, L. N.; Zhao, Y.; Peng, W.; Murali, B.; Sarmah, S. P.; Yuan, M.; Sinatra, L.; Alyami, N. M.; Liu, J. Highly Efficient Perovskite-Quantum-Dot Light-Emitting Diodes by Surface Engineering. *Adv. Mater.* **2016**, *28*, 8718−8725.
(43) Pan, J.; Sarmah, S. P.; Murali, B.; Dursun, I.; Peng, W.; Parida, M. R.; Liu, J.; Sinatra, L.; Alyami, N.; Zhao, C.; et al. Air-Stable Surface-Passivated Perovskite Quantum Dots for Ultra-Robust, Single- and Two-Photon-Induced Amplified Spontaneous Emission. *J. Phys. Chem. Lett.* **2015**, *6*, 5027−5033.
(44) Imran, M.; Ijaz, P.; Baranov, D.; Goldoni, L.; Petralanda, U.; Akkerman, Q.; Abdelhady, A. L.; Prato, M.; Bianchini, P.; Infante, I.; et al. Shape-Pure, Nearly Monodispersed $CsPbBr_3$ Nanocubes Prepared Using Secondary Aliphatic Amines. *Nano Lett.* **2018**, *18*, 7822−7831.
(45) Vickers, E. T.; Graham, T. A.; Chowdhury, A. H.; Bahrami, B.; Dreskin, B. W.; Lindley, S.; Naghadeh, S. B.; Qiao, Q.; Zhang, J. Z. Improving Charge Carrier Delocalization in Perovskite Quantum Dots by Surface Passivation with Conductive Aromatic Ligands. *ACS Energy Lett.* **2018**, *3*, 2931−2939.
(46) Krieg, F.; Ochsenbein, S. T.; Yakunin, S.; Ten Brinck, S.; Aellen, P.; Süess, A.; Clerc, B.; Guggisberg, D.; Nazarenko, O.; Shynkarenko, Y. Colloidal $CsPbX_3$ (X= Cl, Br, I) Nanocrystals 2.0: Zwitterionic Capping Ligands for Improved Durability and Stability. *ACS Energy Lett.* **2018**, *3*, 641−646.
(47) Lee, S.; Park, J. H.; Lee, B. R.; Jung, E. D.; Yu, J. C.; Di Nuzzo, D.; Friend, R. H.; Song, M. H. Amine-Based Passivating Materials for Enhanced Optical Properties and Performance of Organic−Inorganic Perovskites in Light-Emitting Diodes. *J. Phys. Chem. Lett.* **2017**, *8*, 1784−1792.
(48) Nenon, D. P.; Pressler, K.; Kang, J.; Koscher, B. A.; Olshansky, J. H.; Osowiecki, W. T.; Koc, M. A.; Wang, L.-W.; Alivisatos, A. P. Design Principles for Trap-Free $CsPbX_3$ Nanocrystals: Enumerating and Eliminating Surface Halide Vacancies with Softer Lewis Bases. *J. Am. Chem. Soc.* **2018**, *140*, 17760−17772.
(49) Parobek, D.; Roman, B. J.; Dong, Y.; Jin, H.; Lee, E.; Sheldon, M.; Son, D. H. Exciton-to-Dopant Energy Transfer in Mn-Doped Cesium Lead Halide Perovskite Nanocrystals. *Nano Lett.* **2016**, *16*, 7376−7380.
(50) Liu, W.; Lin, Q.; Li, H.; Wu, K.; Robel, I.; Pietryga, J. M.; Klimov, V. I. Mn^{2+}-Doped Lead Halide Perovskite Nanocrystals with Dual-Color Emission Controlled by Halide Content. *J. Am. Chem. Soc.* **2016**, *138*, 14954−14961.
(51) Guria, A. K.; Dutta, S. K.; Adhikari, S. D.; Pradhan, N. Doping Mn^{2+} in Lead Halide Perovskite Nanocrystals: Successes and Challenges. *ACS Energy Lett.* **2017**, *2*, 1014−1021.
(52) Hu, Q.; Li, Z.; Tan, Z.; Song, H.; Ge, C.; Niu, G.; Han, J.; Tang, J. Rare Earth Ion-Doped $CsPbBr_3$ Nanocrystals. *Adv. Opt. Mater.* **2018**, *6*, 1700864.
(53) Song, E.; Ding, S.; Wu, M.; Ye, S.; Chen, Z.; Ma, Y.; Zhang, Q. Tunable White Upconversion Luminescence from Yb^{3+}-Tm^{3+}-Mn^{2+} Tri-Doped Perovskite Nanocrystals. *Opt. Mater. Express* **2014**, *4*, 1186−1196.
(54) Pan, G.; Bai, X.; Yang, D.; Chen, X.; Jing, P.; Qu, S.; Zhang, L.; Zhou, D.; Zhu, J.; Xu, W.; et al. Doping Lanthanide into Perovskite Nanocrystals: Highly Improved and Expanded Optical Properties. *Nano Lett.* **2017**, *17*, 8005−8011.
(55) Mir, W. J.; Mahor, Y.; Lohar, A.; Jagadeeswararao, M.; Das, S.; Mahamuni, S.; Nag, A. Postsynthesis Doping of Mn and Yb into $CsPbX_3$ (X= Cl, Br, or I) Perovskite Nanocrystals for Downconversion Emission. *Chem. Mater.* **2018**, *30* (22), 8170−8178.
(56) Wang, L.; Zhou, H.; Hu, J.; Huang, B.; Sun, M.; Dong, B.; Zheng, G.; Huang, Y.; Chen, Y.; Li, L.; et al. A Eu^{3+}-Eu^{2+} Ion Redox Shuttle Imparts Operational Durability to Pb-I Perovskite Solar Cells. *Science* **2019**, *363*, 265−270.
(57) van der Stam, W.; Geuchies, J. J.; Altantzis, T.; van den Bos, K. H. W.; Meeldijk, J. D.; Van Aert, S.; Bals, S.; Vanmaekelbergh, D.; de Mello Donega, C. Highly Emissive Divalent-Ion-Doped Colloidal $CsPb_{1-x}M_xBr_3$ Perovskite Nanocrystals through Cation Exchange. *J. Am. Chem. Soc.* **2017**, *139*, 4087−4097.
(58) Zou, S.; Liu, Y.; Li, J.; Liu, C.; Feng, R.; Jiang, F.; Li, Y.; Song, J.; Zeng, H.; Hong, M.; et al. Stabilizing Cesium Lead Halide Perovskite Lattice through Mn(II) Substitution for Air-Stable Light-Emitting Diodes. *J. Am. Chem. Soc.* **2017**, *139*, 11443−11450.
(59) Begum, R.; Parida, M. R.; Abdelhady, A. L.; Murali, B.; Alyami, N. M.; Ahmed, G. H.; Hedhili, M. N.; Bakr, O. M.; Mohammed, O. F. Engineering Interfacial Charge Transfer in $CsPbBr_3$ Perovskite Nanocrystals by Heterovalent Doping. *J. Am. Chem. Soc.* **2017**, *139*, 731−737.
(60) Milstein, T. J.; Kroupa, D. M.; Gamelin, D. R. Picosecond Quantum Cutting Generates Photoluminescence Quantum Yields Over 100% in Ytterbium-Doped $CsPbCl_3$ Nanocrystals. *Nano Lett.* **2018**, *18*, 3792−3799.
(61) Yong, Z.-J.; Guo, S.-Q.; Ma, J.-P.; Zhang, J.-Y.; Li, Z.-Y.; Chen, Y.-M.; Zhang, B.-B.; Zhou, Y.; Shu, J.; Gu, J.-L.; et al. Doping-Enhanced Short-Range Order of Perovskite Nanocrystals for Near-Unity Violet Luminescence Quantum Yield. *J. Am. Chem. Soc.* **2018**, *140*, 9942−9951.
(62) Bi, C.; Wang, S.; Li, Q.; Kershaw, S. V.; Tian, J.; Rogach, A. L. Thermally Stable Copper(II)-Doped Cesium Lead Halide Perovskite Quantum Dots with Strong Blue Emission. *J. Phys. Chem. Lett.* **2019**, *10*, 943−952.
(63) Woo, J. Y.; Kim, Y.; Bae, J.; Kim, T. G.; Kim, J. W.; Lee, D. C.; Jeong, S. Highly Stable Cesium Lead Halide Perovskite Nanocrystals through in Situ Lead Halide Inorganic Passivation. *Chem. Mater.* **2017**, *29*, 7088−7092.
(64) Shen, X.; Zhang, Y.; Kershaw, S. V.; Li, T.; Wang, C.; Zhang, X.; Wang, W.; Li, D.; Wang, Y.; Lu, M.; et al. Zn-Alloyed $CsPbI_3$ Nanocrystals for Highly Efficient Perovskite Light-Emitting Devices. *Nano Lett.* **2019**, *19*, 1552.
(65) Mondal, N.; De, A.; Samanta, A. Achieving Near-Unity Photoluminescence Efficiency for Blue-Violet-Emitting Perovskite Nanocrystals. *ACS Energy Lett.* **2019**, *4*, 32−39.
(66) Ball, J. M.; Petrozza, A. Defects in Perovskite-Halides and Their Effects in Solar Cells. *Nat. Energy* **2016**, *1*, 16149.
(67) Nayak, P. K.; Sendner, M.; Wenger, B.; Wang, Z.; Sharma, K.; Ramadan, A. J.; Lovrinčić, R.; Pucci, A.; Madhu, P. K.; Snaith, H. J. Impact of Bi^{3+} Heterovalent Doping in Organic−Inorganic Metal Halide Perovskite Crystals. *J. Am. Chem. Soc.* **2018**, *140*, 574−577.
(68) Lozhkina, O. A.; Murashkina, A. A.; Shilovskikh, V. V.; Kapitonov, Y. V.; Ryabchuk, V. K.; Emeline, A. V.; Miyasaka, T. Invalidity of Band-Gap Engineering Concept for Bi^{3+} Heterovalent Doping in $CsPbBr_3$ Halide Perovskite. *J. Phys. Chem. Lett.* **2018**, *9*, 5408−5411.
(69) Yao, J.-S.; Ge, J.; Han, B.-N.; Wang, K.-H.; Yao, H.-B.; Yu, H.-L.; Li, J.-H.; Zhu, B.-S.; Song, J.-Z.; Chen, C.; et al. Ce^{3+}-Doping to Modulate Photoluminescence Kinetics for Efficient $CsPbBr_3$ Nanocrystals Based Light-Emitting Diodes. *J. Am. Chem. Soc.* **2018**, *140*, 3626−3634.
(70) Yin, J.; Ahmed, G. H.; Bakr, O. M.; Brédas, J.-L.; Mohammed, O. F. Unlocking the Effect of Trivalent Metal Doping in All-Inorganic $CsPbBr_3$ Perovskite. *ACS Energy Lett.* **2019**, *4*, 789−795.
(71) Di Stasio, F.; Christodoulou, S.; Huo, N.; Konstantatos, G. Near-Unity Photoluminescence Quantum Yield in $CsPbBr_3$ Nanocrystal Solid-State Films via Postsynthesis Treatment with Lead Bromide. *Chem. Mater.* **2017**, *29*, 7663−7667.
(72) Li, F.; Liu, Y.; Wang, H.; Zhan, Q.; Liu, Q.; Xia, Z. Postsynthetic Surface Trap Removal of $CsPbX_3$ (X = Cl, Br, or I) Quantum Dots via a ZnX_2/Hexane Solution toward an Enhanced Luminescence Quantum Yield. *Chem. Mater.* **2018**, *30*, 8546−8554.
(73) Abdi-Jalebi, M.; Andaji-Garmaroudi, Z.; Cacovich, S.; Stavrakas, C.; Philippe, B.; Richter, J. M.; Alsari, M.; Booker, E. P.; Hutter, E. M.; Pearson, A. J.; et al. Maximizing and Stabilizing Luminescence from Halide Perovskites with Potassium Passivation. *Nature* **2018**, *555*, 497.

DOI: 10.1021/acs.jpclett.9b00689
J. Phys. Chem. Lett. 2019, 10, 2629−2640

(74) Ahmed, G. H.; El-Demellawi, J. K.; Yin, J.; Pan, J.; Velusamy, D. B.; Hedhili, M. N.; Alarousu, E.; Bakr, O. M.; Alshareef, H. N.; Mohammed, O. F. Giant Photoluminescence Enhancement in $CsPbCl_3$ Perovskite Nanocrystals by Simultaneous Dual-Surface Passivation. *ACS Energy Lett.* **2018**, *3*, 2301−2307.
(75) Lu, M.; Zhang, X.; Zhang, Y.; Guo, J.; Shen, X.; Yu, W. W.; Rogach, A. L. Simultaneous Strontium Doping and Chlorine Surface Passivation Improve Luminescence Intensity and Stability of $CsPbI_3$ Nanocrystals Enabling Efficient Light-Emitting Devices. *Adv. Mater.* **2018**, *30*, 1804691.
(76) Ke, W.; Xiao, C.; Wang, C.; Saparov, B.; Duan, H. S.; Zhao, D.; Xiao, Z.; Schulz, P.; Harvey, S. P.; Liao, W. Employing Lead Thiocyanate Additive to Reduce the Hysteresis and Boost the Fill Factor of Planar Perovskite Solar Cells. *Adv. Mater.* **2016**, *28*, 5214−5221.
(77) Chiang, Y.-H.; Li, M.-H.; Cheng, H.-M.; Shen, P.-S.; Chen, P. Mixed Cation Thiocyanate-Based Pseudohalide Perovskite Solar Cells with High Efficiency and Stability. *ACS Appl. Mater. Interfaces* **2017**, *9*, 2403−2409.
(78) Jiang, Q.; Rebollar, D.; Gong, J.; Piacentino, E. L.; Zheng, C.; Xu, T. Pseudohalide-Induced Moisture Tolerance in Perovskite $CH_3NH_3Pb(SCN)_2I$ Thin Films. *Angew. Chem., Int. Ed.* **2015**, *54*, 7617−7620.
(79) Yu, Y.; Wang, C.; Grice, C. R.; Shrestha, N.; Chen, J.; Zhao, D.; Liao, W.; Cimaroli, A. J.; Roland, P. J.; Ellingson, R. J. Improving the Performance of Formamidinium and Cesium Lead Triiodide Perovskite Solar Cells Using Lead Thiocyanate Additives. *ChemSusChem* **2016**, *9*, 3288−3297.
(80) Yu, Y.; Wang, C.; Grice, C. R.; Shrestha, N.; Zhao, D.; Liao, W.; Guan, L.; Awni, R. A.; Meng, W.; Cimaroli, A. J. Synergistic Effects of Lead Thiocyanate Additive and Solvent Annealing on the Performance of Wide-Bandgap Perovskite Solar Cells. *ACS Energy Lett.* **2017**, *2*, 1177−1182.
(81) Pham, N. D.; Tiong, V. T.; Yao, D.; Martens, W.; Guerrero, A.; Bisquert, J.; Wang, H. Guanidinium Thiocyanate Selective Ostwald Ripening Induced Large Grain for High Performance Perovskite Solar Cells. *Nano Energy* **2017**, *41*, 476−487.
(82) Koscher, B. A.; Swabeck, J. K.; Bronstein, N. D.; Alivisatos, A. P. Essentially Trap-Free $CsPbBr_3$ Colloidal Nanocrystals by Postsynthetic Thiocyanate Surface Treatment. *J. Am. Chem. Soc.* **2017**, *139*, 6566−6569.
(83) Leng, M.; Yang, Y.; Chen, Z.; Gao, W.; Zhang, J.; Niu, G.; Li, D.; Song, H.; Zhang, J.; Jin, S.; et al. Surface Passivation of Bismuth-Based Perovskite Variant Quantum Dots To Achieve Efficient Blue Emission. *Nano Lett.* **2018**, *18*, 6076−6083.
(84) Behera, R. K.; Das Adhikari, S.; Dutta, S. K.; Dutta, A.; Pradhan, N. Blue-Emitting $CsPbCl_3$ Nanocrystals: Impact of Surface Passivation for Unprecedented Enhancement and Loss of Optical Emission. *J. Phys. Chem. Lett.* **2018**, *9*, 6884−6891.
(85) Wu, Y.; Wei, C.; Li, X.; Li, Y.; Qiu, S.; Shen, W.; Cai, B.; Sun, Z.; Yang, D.; Deng, Z.; et al. In Situ Passivation of $PbBr_6^{4-}$ Octahedra toward Blue Luminescent $CsPbBr_3$ Nanoplatelets with Near 100% Absolute Quantum Yield. *ACS Energy Lett.* **2018**, *3*, 2030−2037.
(86) Reiss, P.; Protière, M.; Li, L. Core/Shell Semiconductor Nanocrystals. *Small* **2009**, *5*, 154−168.
(87) Sun, C.; Zhang, Y.; Ruan, C.; Yin, C.; Wang, X.; Wang, Y.; Yu, W. W. Efficient and Stable White LEDs with Silica-Coated Inorganic Perovskite Quantum Dots. *Adv. Mater.* **2016**, *28*, 10088−10094.
(88) Xu, K.; Lin, C. C.; Xie, X.; Meijerink, A. Efficient and Stable Luminescence from Mn^{2+} in Core and Core−Isocrystalline Shell $CsPbCl_3$ Perovskite Nanocrystals. *Chem. Mater.* **2017**, *29*, 4265−4272.
(89) Liu, J.; Song, K.; Shin, Y.; Liu, X.; Chen, J.; Yao, K. X.; Pan, J.; Yang, C.; Yin, J.; Xu, L.-J.; et al. Light-Induced Self-Assembly of Cubic $CsPbBr_3$ Perovskite Nanocrystals into Nanowires. *Chem. Mater.* **2019**, DOI: 10.1021/acs.chemmater.9b00680.
(90) Ma, J.-P.; Chen, Y.-M.; Zhang, L.-M.; Guo, S.-Q.; Liu, J.-D.; Li, H.; Ye, B.-J.; Li, Z.-Y.; Zhou, Y.; Zhang, B.-B.; et al. Insights into the Local Structure of Dopants, Doping Efficiency, and Luminescence Properties of Lanthanide-Doped $CsPbCl_3$ Perovskite Nanocrystals. *J. Mater. Chem. C* **2019**, *7*, 3037−3048.

DOI: 10.1021/acs.jpclett.9b00689
J. Phys. Chem. Lett. 2019, 10, 2629−2640